

USING REMOTE MONITORING AND MACHINE LEARNING TO CLASSIFY SLAM EVENTS OF WAVE PIERCING CATAMARANS

B Shabani, J Ali-Lavroff, D S Holloway, University of Tasmania, Australia, **S Penev**, UNSW Sydney, Australia, **D Dessi**, Italian National Research Council, Italy, **G Thomas**, University College London, UK

SUMMARY

An onboard monitoring system can measure features such as stress cycles counts and provide warnings due to slamming. Considering current technology trends there is the opportunity of incorporating machine learning methods into monitoring systems. A hull monitoring system has been developed and installed on a 111 m wave piercing catamaran (Hull 091) to remotely monitor the ship kinematics and hull structural responses. Parallel to that, an existing dataset of a similar vessel (Hull 061) was analysed using unsupervised and supervised learning models; these were found to be beneficial for the classification of bow entry events according to key kinematic parameters. A comparison of different algorithms including linear support vector machines, naïve Bayes and decision tree for the bow entry classification were conducted. In addition, using empirical probability distributions, the likelihood of wet-deck slamming was estimated given a vertical bow acceleration threshold of 1 g in head seas, clustering the feature space with the approximate probabilities of 0.001, 0.030 and 0.25.

1. INTRODUCTION

Wet-deck slamming (wave impact against the cross-deck structure) is an important consideration in the structural design of catamarans (Lavroff *et al.*, 2013, Shabani *et al.*, 2018a). The centre bow (shown in Figures 1 and 2) minimises the risk of deck-diving and improves seakeeping characteristics but adds complexity and non-linearity in the hull-wave interaction during arch filling and wet-deck slamming (Lavroff and Davis, 2015). Large transient slam loads may occur, generating whipping and structural vibrations (Thomas *et al.*, 2011) and in the long term, these vibrations can contribute to fatigue (Amin *et al.*, 2013).



Figure 1: HSV-2 SWIFT, a 98-meter wave piercing catamaran built in 2003 (Hull 061) (Incat.com.au, 2019).

The severity of slam forces on high speed wave piercing catamarans (WPCs) has been reported to be in the order of the vessel weight but a high level of uncertainty still exists in determining these loads. There have been numerical simulations of motions and loads of WPCs (McVicar *et al.*, 2018) and model test programmes for measuring the extreme model scale loads with respect to various speeds and wave heights in both regular and irregular waves (Davis *et al.*, 2017, Lavroff *et al.*, 2017, AlaviMehr *et al.*, 2019). Recent studies on motions and

loads of WPCs have been based on hydroelastic segmented model tests mainly conducted in regular (Shabani *et al.*, 2019b, c, d) and irregular (Davis *et al.*, 2017) head waves.



Figure 2: Volcan De Tagoro, A 111- m wave piercing catamaran built in 2019 (Hull 091) (Incat.com.au, 2019).



Figure 3: The centre bow of a model wave piercing catamaran (Shabani *et al.*, 2017).

Slam loads, pressures and kinematics of WPCs during bow entry events in regular head seas were investigated previously in (Shabani *et al.*, 2017, Shabani *et al.*, 2018a, Shabani *et al.*, 2018b, Shabani *et al.*, 2019a, Shabani *et al.*, 2019b, c, d). In regular waves, it was seen that wet-deck slamming occurs when the centre bow (see Figure 3) immersion depth relative to undisturbed water surface reaches a certain limit which is a function of wave encounter frequency. This is shown in Figure 4 for two dimensionless wave encounter frequencies. In real operating conditions, a large set of data can lead to more accurate predictions of wet-deck slamming events. This is important from a structural design perspective considering that the existing prediction methods and design rules for WPCs are yet to be fully developed.

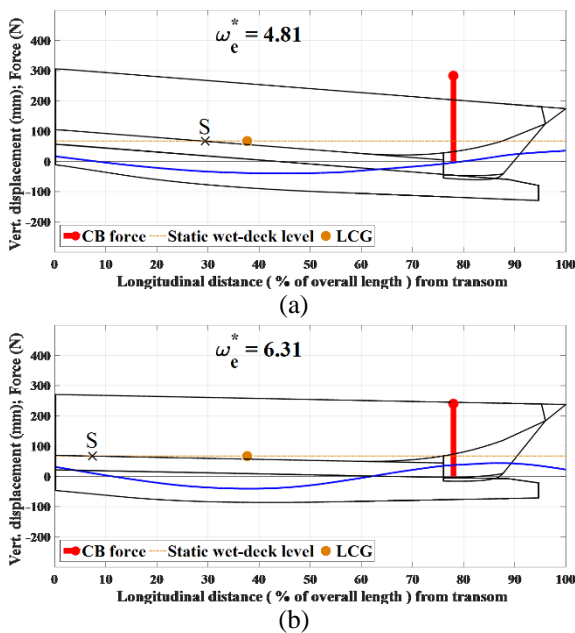


Figure 4: Vertical displacement, encountered wave profile and centre bow (CB) load at slamming instants for a catamaran model in $h_w = 90$ mm, $V_m = 2.89$ m/s for two dimensionless wave encounter frequencies (ω_e^*). 'S' shows intersection point of the static wet-deck level and instantaneous wet-deck line, h_w is wave height and V_m is the model velocity (Shabani *et al.*, 2018a).

A hull monitoring system, which integrates strain gauges, accelerometers and other sensors, can provide valuable information for both ship design and operations. A monitoring system can have standard features specified in class guidelines such as stress cycles counts, warnings due to slamming and excessive motions. Considering the current technology trends and digitalisation affecting services, products and processes, smart and connected hull monitoring systems incorporating machine learning (ML) and deep learning methods are of interest (Bekker *et al.*, 2018).

When it comes to slamming, a hull monitoring system could be developed in order to satisfy multiple

requirements in real-time. For example, it may have certain features to (1) predict ahead of time if the vessel is likely to be subjected to wave impacts given the current operating conditions (2) provide awareness of the likelihood and severity of slamming events that could hypothetically lead to either local or global structural damage (3) propose a modified speed or change of course to minimise the structural risks (4) automatically identify slamming events and provide a statistical summary of slamming occurrences and severity according to slam-induced accelerations and hull stresses. The first three features mentioned above represent some of the problems that were addressed by Ochi and Motter (Ochi and Motter, 1973) through a closed-form statistical model. More details of the Ochi slamming conditions and slamming probability can be found in (Dessi and Ciappi, 2013) and a review of slamming identification methods can be also found in (Magoga *et al.*, 2017). Nevertheless, the alternative methods based on ML have yet to be developed to identify and classify slamming events in random waves.

Various ML techniques (Aghabozorgi *et al.*, 2015, Jain *et al.*, 1999, Mahdavinejad *et al.*, 2018, Witten *et al.*, 2016, Berkhin, 2006) have been developed to address a variety of classification problems. Among a broad range of applications, ML models for structural health monitoring, damage detection and predictive maintenance of mechanical systems, ships and offshore structures (Mitra and Gopalakrishnan, 2016) and digital twin of a research vessel (Bekker, 2018) can be highlighted.

In this paper, the development of a remote monitoring system will be presented, and machine learning algorithms will be applied to classify centre bow entry events in random seas. This is part of a broader research project which aims to develop smart and connected hull monitoring systems specific to WPCs.

2. FULL-SCALE DATASETS

2.1 HULL 091 MONITORING SYSTEM

A hull monitoring system has been developed for Hull 091 Incat vessel (see Figure 2). The vessel was instrumented in July 2019 using a motion reference unit (MRU), a bow accelerometer and 10 strain gauges. An ultrasonic wave sensor was placed in the bow area to measure the incident wave profiles. An overview of the remote monitoring system is shown in Table 1. Figure 5 shows the approximate longitudinal locations of the cDAQ, laptop, MRU, strain gauges, bow accelerometer and the ultrasonic sensor. The sampling rates were not consistent across the sensors because of the requirements of modules/sensors. More specifically, the sampling rates were set to 1000 Hz for strain gauge data, 100 Hz for the bow and MRU acceleration data, 50 Hz for MRU heave, pitch and roll data and 9 Hz for the ultrasonic sensor.

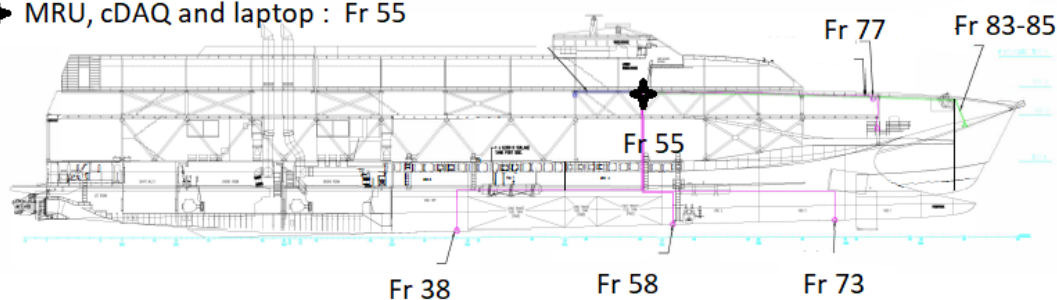
A LabVIEW program was developed to record and upload data automatically to a Google Drive account given a set of predefined rules and triggers. For instance, the LabVIEW program records full raw data as a technical data management streaming (TDMS) file and creates a subset file when the bow vertical acceleration

is above 0.5g with a window of 30 seconds. In addition, the rain flow counting algorithm available in LabVIEW was included to output a comma-separated values (CSV) file, providing a summary of strain cycle counts from each strain gauge.

Table 1 Overview of Hull 091 remote monitoring components

Category	Item	Quantity	Description
Sensors /data source	Strain gauges	10	HBM 1-LY43-6/350
	Accelerometer (3-axial)	1	CrossBow- CXL04GP3
	Ultrasonic sensor	1	ToughSonic 50(TSPC-21SRM-485)
	Motion reference unit (MRU)	1	SBG Systems- Ellipse2-A
	Global Positioning System (GPS) receiver	1	Hull 091 GPS distributor
Data acquisition	Data acquisition (DAQ) module	1	National Instrument (NI cDAQ-9174)
	Strain gauges module (8 channel)	2	National Instrument (NI-9236)
	Universal Input module (4 channel)	1	National Instrument (NI-9219)
Computer, accessories and software	Laptop	1	Dell latitude 7490
	USB Hub	1	Powered USB hub
	Onboard Monitoring Software	1	Customised LabVIEW program
	Remote Desktop Access	1	TeamViewer
	Laptop tray	1	RAM Universal tray (RAM-234-3)
	Cabinet	1	PCLocs – Carrier 10
Storage & connectivity	NMEA to USB convertor	1	Digital Yacht
	External hard drive	1	Samsung- USB-C 1T SSD
	Cloud based storage	100GB (scalable)	Google Drive
	WiFi/LAN router	1	Digital Yacht 4G Connect PRO
	4G antennas	2	Digital Yacht 4G Connect PRO
	Sim Card	1	Simyo 4G

✦ MRU, cDAQ and laptop : Fr 55



Strain gauges: Fr 38, 58, 73, 77 & 83 Bow accelerometer & ultrasonic sensor: Fr 83-85

Figure 5: Hull 091 cabling diagram from Frame 55 to frames (Fr) 38, 58, 73, 77, 83 and 85, showing the approximate longitudinal locations of the cDAQ, laptop, MRU, strain gauges, bow accelerometer and ultrasonic sensor listed in Table 1.

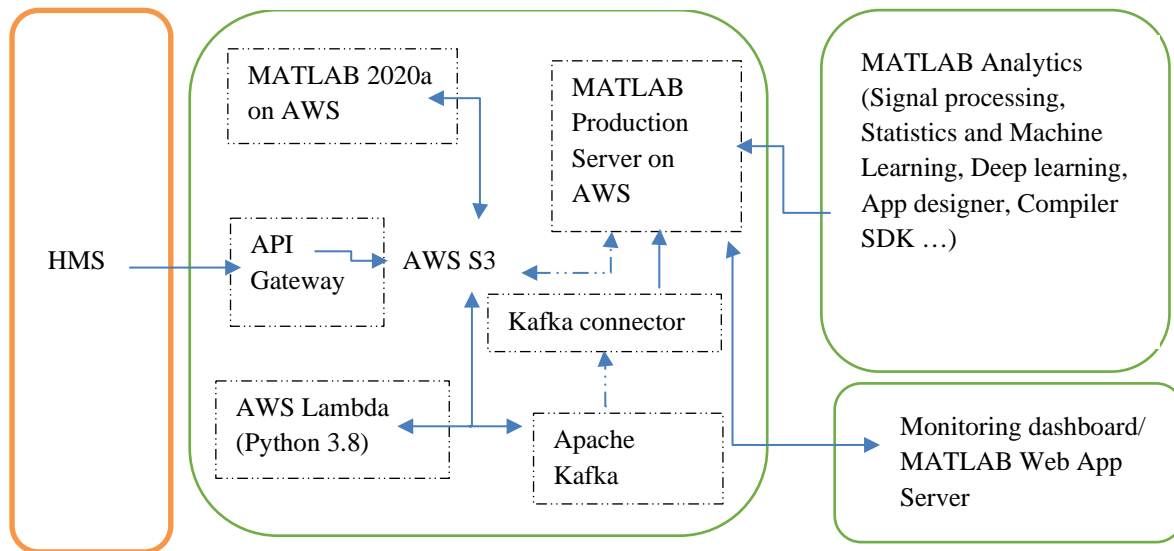


Figure 6: A sample streaming architecture, presenting data analytic & visualisation resources for a remote hull monitoring system (HMS) using Amazon Web Services (AWS) and MathWorks product

It is worth mentioning that developing a customised LabVIEW program enabled the integration of the MRU and GPS data. This was achieved by incorporating SBG Systems (Ellipse2-A) and NMEA-0183 GPS drivers, to the strain gauges, bow accelerometer and ultrasonic sensor data acquired from NI 9236 and 9219 modules. Furthermore, a file management function was included so that the files could be uploaded into the Google Drive and deleted from the computer hard drive. The choice of Google Drive here is due to having a general purpose, temporary storage for preliminary data access and some other user-friendly features such as automatic synchronisation and backup to manage large data files. Password and two-step verification mechanisms were enabled to protect data and enhance security of the remote access to the monitoring computer.

The customised upload code developed in the LabVIEW program can be adjusted to upload the data into a cloud platform which enables advanced features such as machine learning, deep learning and near real-time monitoring. Such features, for example, are available in public cloud computing services such as Amazon Web Services (AWS) Google Cloud Platform (GCP), and Microsoft Azure.

Figure 6 shows a typical streaming architecture, presenting data analytic and visualisation resources considered for the remote hull monitoring system. Through an Application Programming Interface (API), the solution architecture allows access to AWS data storage service (i.e. S3), sending information to AWS Lambda for serverless processing and using MATLAB on AWS for parallel computing. It also enables MATLAB users using different MATLAB runtimes to develop their algorithms on a local machine by incorporating some essential modules such as signal

processing, machine learning and statistics or deep learning toolboxes but compile their codes to be deployed on MATLAB production server. The production server consists of several MATLAB workers running on remote computing instances on AWS and supports analytic integration to third-party software and webpages. The architecture incorporates Apache Kafka (i.e. a distributed streaming platform) for real time analytics. In addition, through web app designer and web app server, MATLAB applications can be designed and deployed to enable signal monitoring and customised analytics. At the time of writing this document, the data workflow benefits from AWS S3, and MATLAB on AWS for signal preprocessing and filtering, standard calculations such as cumulative strain cycle counts on a monthly basis and reporting Motion Sickness Incidence (MSI) of voyages in each month. MSIs were calculated using rms weighted vertical accelerations for the location at which the MRU was placed. A Lambda function was also developed to highlight the highest peak bow acceleration of each month automatically on AWS (i.e. based on trigger events defined by new files received in S3 and without managing compute infrastructure). A customised MATLAB application was also developed to visualise the processed data. However, machine learning algorithms and near real-time analytics are yet to be investigated.

Table 2 Main particulars of Hull 091 and Hull 061

	Hull 091	Hull 061
Length overall	111.9 m	97.22 m
Length waterline	103.2 m	92 m
Beam Overall	30.5	26.6 m
Draught	4.1 m	3.434 m
Demihull beam	5.8 m	4.5 m
Max Deadweight	1000 tonnes	670 tonnes
Speed	42.4 knots	38 knots

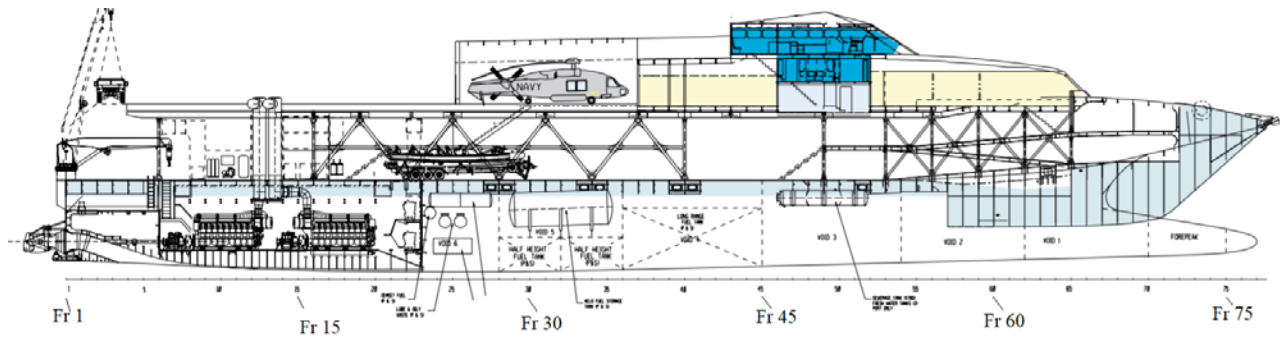


Figure 7: General arrangement (GA) of Hull 061.

Table 3 An overview of HSV-2 Swift (Hull 061) seakeeping and structural loads data obtained from sea trials between 11th and 17th of May 2004

Total Runs	Sea State	Significant Wave Height (m)	Ship Speed (knots)	Number of channels	Sampling rate	Total data rows
159	4-5	1.8- 3.8	10-38	79	100 Hz	24 million

Table 4 Selected runs in head seas for Hull 061 data series

Run number	Significant wave height (m)	Modal period (s)	Speed (knots)	Ride control status	Run duration (min.)
70	2.4	8.2	20	ON	21.1
92	3.0	11	30	ON	22.2
99	2.0	7.5	35	OFF	19.4
145	2.4	10.2	35	ON	19.5
159	1.7	8.4	30	OFF	20.2
174	2.9	10.2	35	ON	20.4
180	2.8	9.7	35	OFF	20.3
192	1.9	7.6	30	ON	19.7
206	1.6	7.2	15	OFF	21.1

The delivery voyage of Hull 091 from Hobart, Tasmania to Canary Islands, Spain took place between 15 July and 15 August 2019 and over 200 GB data has been collected so far. Hull 061 sea trials data was first used in order to develop a classification algorithm for the bow entry of high-speed WPCs. Table 2 compares main particulars of Hull 061 and Hull 091.

2.2 DEVELOPMENT OF ML PIPELINE USING EXISTING HULL 061 DATA

An existing dataset (Hull 061 dataset) was used to propose a possible architecture for an ML pipeline, in which ML workflows can be automated as described in Figure 6. The use of Hull 061 dataset was an important step given the fact that the two vessels are similar in

design, noting that the main objective of the ML workflows in this work is to classify the bow entry events according to the kinematics of centre bow entry (Shabani *et al.*, 2018a) in random waves. In addition, the successful instrumentation of Hull 061 and notable findings regarding slamming characteristics were the key for developing a remote monitoring system for Hull 091. The choice of having an ML model developed for classifying bow entry events of Hull 091 in the present work is also linked to Hull 061 bow entry events which resulted in wet-deck slamming occurrences (Jacobi *et al.*, 2012, Jacobi *et al.*, 2014) in various speeds and wave heights during HSV-2 Swift sea trials.

The seakeeping and structural loads trials of Hull 061 were conducted in May 2004. The vessel was extensively instrumented by 47 strain gauges and 4

triaxial accelerometers located at the bow, bridge, LCG, and flight deck. The roll, pitch and yaw were measured at the longitudinal centre of gravity and a Tsurumi Seiki Co. Ltd (TSK) wave height meter system was installed at Fr 72 (see Figure 7). Several parameters of the shipboard control systems were also monitored including the position of the T-foil and trim tabs, waterjet nozzle angle and waterjet shaft speed. Table 3 shows an overview of Hull 061 seakeeping and structural loads data obtained from sea trials between 11th and 17th of May 2004. The accumulated data rows from all runs were approximately 24 million rows, an equivalent of 66.6 hours of logged data at 100 Hz.

The sea trials were conducted in various wave heights and different octagons, each with five legs from head seas to following seas at a constant ship speed throughout each octagon. Since head seas accounted for a larger number of slams in comparison to other headings (Jacobi *et al.*, 2014), a total of 9 runs in head seas were selected for current analyses as listed in Table 4.

3. DATA ANALYSES APPROACH

3.1 TIME SERIES SEGMENTATION & FEATURE EXTRACTION

The rate of wet-deck slamming occurrence is a function of the centre bow and wet-deck geometry, speed, wave height and other operational factors (Jacobi *et al.*, 2014), but the condition in which a wet-deck slam can occur is often simplified by considering the relative vertical bow displacements along the centre bow (Davis *et al.*, 2017, Shabani *et al.*, 2018a). The rate of wet-deck slamming occurrence therefore can be described by the number of bow entries exceeding a threshold value (Davis *et al.*, 2017) noting that the variability of the threshold relative vertical bow displacement can be included.

A new approach is proposed in this work with the objective of having an automated data pipeline for describing bow entry events, in particular those that are likely associated with wet-deck slamming events. Figure 8 shows the overall approach proposed for classifying the bow entry events that incorporates unsupervised and supervised classification methods (Witten *et al.*, 2016).

As mentioned earlier, various methods for identification of slamming events have been proposed previously including whipping-based criterion (Dessi, 2014), maximum rate of change of stress (Jacobi *et al.*, 2014, Magoga *et al.*, 2017), and wavelet methods (Amin *et al.*, 2013). The approach proposed in Figure 8 considers bow vertical accelerations, strain gauge measurements and relative motions as the inputs for an unsupervised learning algorithm for the classification of the bow entry events. The selected features have some similarities with those mentioned earlier with respect to slamming identification criteria. The unsupervised model can be used for onboard or cloud-based analyses when other all

inputs are available from the measurements. In addition, a supervised learning model is proposed which only requires the relative motions data to classify the bow entry events. The supervised model is then an alternate solution for simulations of wet-deck slamming analyses in random waves according to the bow entry kinematics.

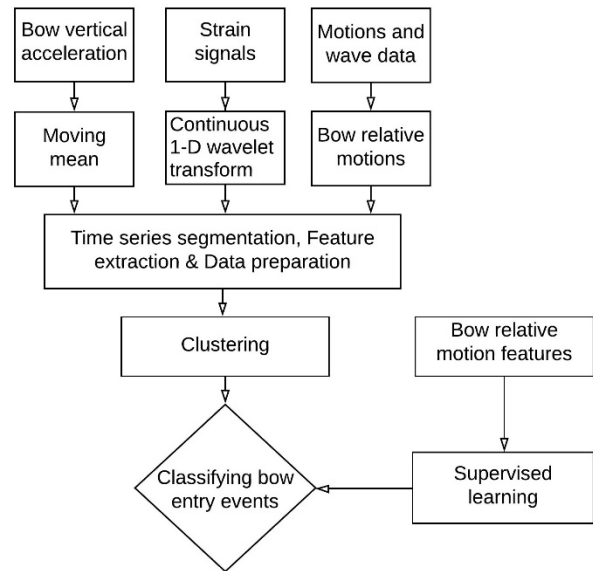


Figure 8: The process of centre bow entry classification.

As shown in Figure 8, in the first step, the moving mean of the bow vertical acceleration was used to divide the time series into segments so that each segment represented a time window between the zero crossings of the moving mean signal (see Figure 9). Only segments with positive moving mean accelerations (see for example Figure 9 between 10.3 and 10.35 minutes) were selected for the analyses as they are linked to the centre bow entry events.

In a parallel step, by parsing strain signals through the 1-D continuous wavelet transform (CWT) function in MATLAB version 2019a (by The MathWorks, Inc.), the frequencies with the highest magnitudes were identified for each strain signal within each segment. The wavelet transform is obtained using the analytic Morse wavelet, with $L1$ normalisation, so equal amplitude oscillatory components in the data at different scales have equal magnitude in the CWT function.

Figure 10 shows an example of the wavelet transform applied to a standardised strain signal, which is scaled to a zero mean and standard deviation of 1. The strain signal was low-pass filtered by a cutoff frequency of 5 Hz before applying the wavelet transform. Frequencies with the highest magnitude are presented as a function of time, showing a peak frequency of 2.83 Hz which plateaued around a time of 14.72 minutes from the start of recording, noting that this was in a segment at which a wet-deck slamming occurred with a peak acceleration of above $2g$.

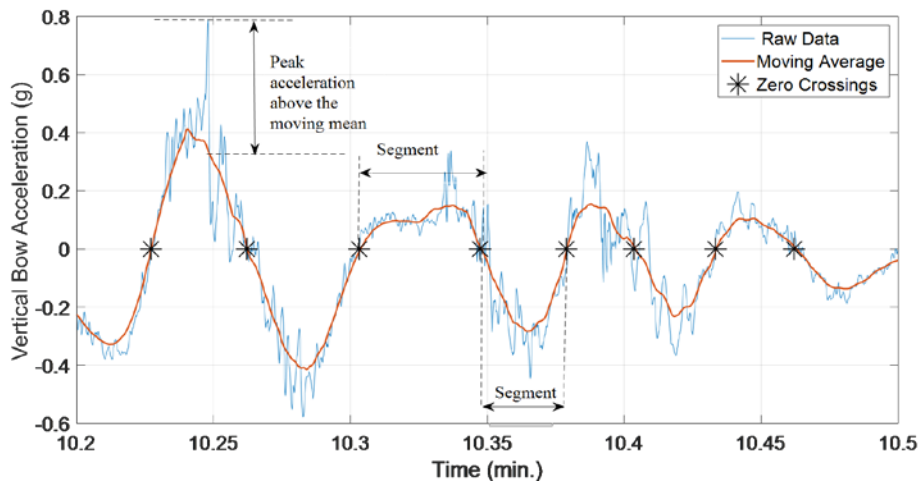


Figure 9: A time record of vertical bow acceleration and its moving average, showing a typical peak acceleration above the mean, and two segments with positive and negative moving mean accelerations. Raw data is taken from Hull 061, Run 145 at a speed of 35 knots in head seas with a significant wave height of 2.4 m.

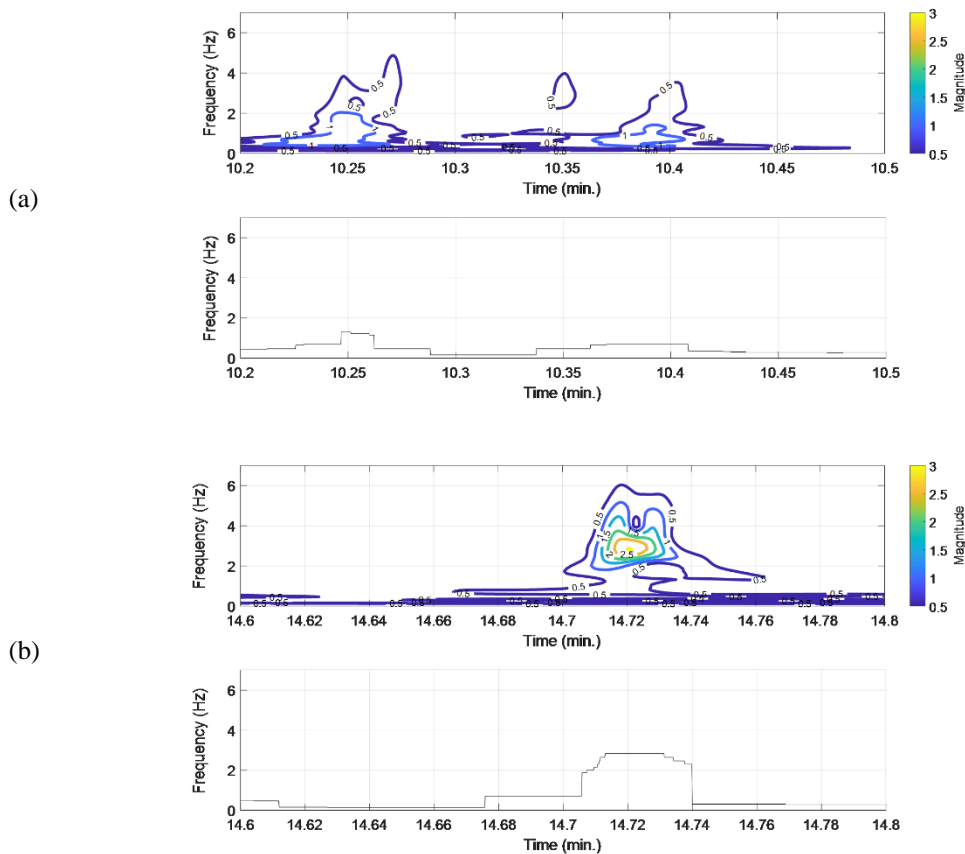


Figure 10: 1-D wavelet transform's frequency and magnitude of a standardised strain signal (contour plots), and frequencies with the highest magnitude as a function of time (line plots): (a) between 10.2 and 10.5 min., corresponding to peak accelerations shown in Figure 9; (b) between 14.6 and 14.8 min., corresponding to an impact with a peak acceleration of above 2g. Raw data is taken from strain gauge T1_10 at Fr 61 measured during Run 145 at a speed of 35 knots in head seas with a significant wave height of 2.4 m. The wavelet transform is obtained using the analytic Morse wavelet. The colour bar shows the magnitude of oscillatory components with **L1** normalisation in MATLAB 2019a.

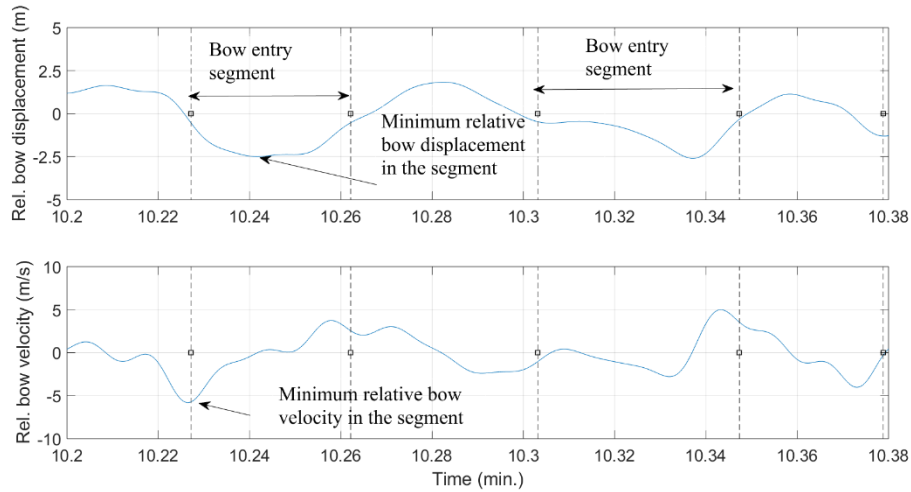


Figure 11: Representation of (a) minimum relative bow displacement in bow entry segments (b) minimum relative bow velocity in bow entry segments. Raw data is taken from Hull 061, Run 145 at a speed of 35 knots in head seas with a significant wave height of 2.4 m.

Table 5 Variables selected for the classification of the centre bow entry

Variable Names	Data category	Selected features	Presentation	Standardisation
<i>var1</i>	Moving average of bow vertical acceleration	Maximum value for each segment	Figure 9	Yes
<i>var2</i>	Vertical bow acceleration above the moving average	Peak value for each segment	Figure 9	Yes
<i>var3</i>	Peak frequencies obtained from the wavelet analyses	Maximum frequency value for each segment	Figure 10	Yes
<i>var4</i>	Peak magnitudes obtained from the wavelet analyses	Maximum magnitude for each segment	Figure 10	Yes
<i>var5</i>	Relative bow displacement	Minimum value for each segment	Figure 11	Yes
<i>var6</i>	Relative bow velocity	Minimum value for each segment	Figure 11	Yes

The centre bow entry in waves was analysed by considering the vertical displacement of the centre bow relative to the measured wave elevation in the bow area. Two parameters were selected to describe the centre bow entry in each segment: (1) relative bow displacement (2) relative bow velocity, as shown in Figure 11. The segment's boundaries in the figure are zero crossing points found by the analyses of the moving average of the vertical bow acceleration as shown in Figure 9. Table 5 shows a summary of features extracted for each segment. Features are either maximum or minimum values of quantities described in Figures 9-11.

In the data preparation step before clustering, features were scaled to have a mean value of zero and a standard deviation of 1. The standardisation function is $Z = \frac{x - \bar{x}}{s}$, where x is sample data, \bar{x} is the mean and s is the standard deviation of the sample data. It is worth noting that the standardisation was conducted after the features listed in Table 5 were calculated from all runs listed in

Table 4. The normalisation is required for the subsequent data clustering (described in the following section) so that the clustering is not biased towards any particular feature.

3.2 DATA CLUSTERING AND SUPERVISED CLASSIFICATION

Data clustering or unsupervised classification is a technique that does not require structured prior information about groups or classes in a given dataset [30]. The objective is to find natural groups (i.e. clusters) within the dataset based on a similarity measure such that each cluster represents a meaningful category according to a selection of variables or features extracted from the original dataset. Various algorithms have been developed for clustering including hierarchical clustering, partitioning and density-based partitioning algorithms [31]. For instance, in the k -means algorithm, which is one of the most widely used methods in partitioning, the objective is to find k clusters from n

observations so that each observation can be assigned to a cluster according to the minimum distance (e.g. Euclidian metric) from the mean value of each cluster (Aghabozorgi *et al.*, 2015, Jain, 2010). While there are various forms of k -means, the main steps are (Jain, 2010, Jain and Dubes, 1988):

Step 1. Select an initial partition with k clusters; repeat steps 2 and 3 until cluster membership stabilises.

Step 2. Generate a new partition by assigning each pattern to its closest cluster centre.

Step 3. Compute new cluster centres

In the steps above the number of clusters (k), distance metric and initialisation of clusters are user specified parameters. Use of the Euclidean distance as the distance metric is a typical choice; other metrics include Manhattan, Chebyshev and Minkowski metrics (Singh *et al.*, 2013). The cluster initialization error can be also minimised through different approaches (Khan and Ahmad, 2004, Likas *et al.*, 2003). It is worth noting that an extension of the basic k -means is the fuzzy c -means (Dunn, 1973, Bezdek, 1981), in which each observation can be assigned to multiple clusters. An in-depth review of the application of clustering techniques can be found in (Dunn, 1973, Bezdek, 1981), noting that the second paper is focused on time series clustering which is the case for the present study.

The clustering analyses were conducted using the statistics and machine learning toolbox available in MATLAB version 2019a, in which a function has been developed that uses a k -means clustering method referred to as Lloyd's algorithm (Lloyd, 1982), but the default setting of the function uses k -means++ (Arthur and Vassilvitskii, 2007). The k -means++ algorithm outperforms Lloyd's algorithm in speed and accuracy by incorporating a different seeding technique that creates k clusters one by one according to a probability function, as opposed to an initial partitioning with k clusters in the first step.

In supervised learning the objective is to train a classifier based on a set of labelled data or training examples. Various classifiers have been developed for this task including Bayesian classifiers, nearest neighbour classifiers, linear and polynomial classifiers, artificial neural networks and decision trees (Kubat, 2017). A review of classification techniques and algorithms with a focus on Internet of Things and sensory data analysis can be found in (Mahdavinejad *et al.*, 2018). In this work, the classification learner application in MATLAB version 2019a was used to train classifiers based on relative motion features.

4. RESULTS

4.1 CLASSIFICATION OF BOW ENTRY EVENTS USING UNSUPERVISED LEARNING

The centre bow entry events were analysed from a total of approximately 3 hours of measurements on Hull 061 accumulated from 9 runs in head seas with a significant wave height in the range between 1.6 m and 3.0 m, as presented in Table 4, in order to classify the events into 3 groups with respect to 6 features listed in Table 5 showing a set of features obtained from strain measurements, vertical bow acceleration and bow relative motion data. The clustering was achieved by using k -means++ algorithm, which was briefly introduced in the previous section. As mentioned earlier, the number of clusters (k) is a user specified parameter and the choice of $k=3$ here can be altered to a higher or lower number. Bow entry events with a minimum relative bow displacement of - 0.5 m at the reference frame of relative motion measurement (i.e. Fr72-Hull 061) were selected. This resulted in a total of 2378 bow entry events, from which 58%, 31% and 11% were identified as "group 1", "group 2" and "group 3", respectively. The differences between the groups can be explained by box plot presentations of feature variables in each group as shown in Figures 12-14. The line inside each box is the median calculated for each distribution, while the upper and lower edges of each box present the 25th and 75th percentiles, respectively. The most extreme data points shown by the upper and lower whiskers correspond approximately to $\pm 2.7\sigma$ if the data were normally distributed, where σ is the standard deviation of the sample population. The data points outside these limits (i.e. 99.3% coverage) are considered as "outliers" and are shown by separate data points in each case.

It can be inferred from Figure 12(b) that group 3 contains strong wet-deck slamming events given the distribution of the outliers in comparison to that in groups 1 and 2. In addition, the likelihood of wet-deck slamming events to be in groups 1 and 2 is much lower than that in group 3, supported by the frequency distributions presented in Figure 13 (a) in which groups 1 and 2 data are almost out of the range of expected whipping frequency (i.e. 2 -3 Hz) for Hull 061. It should be noted that since filtering was not carried out on strain signals prior to the wavelet analyses, unlike group 3, group 1 and 2 data represent bow entry events where global loads are dominant rather than slam-induced whipping loads.

For the above reasons, it can be argued that the kinematics conditions for wet-deck slamming occurrences in terms of bow relative displacement and velocity are best described by group 3 distributions plotted in Figure 14. However, it is difficult to draw a conclusion for conditions leading to wet-deck slamming occurrences based on the individual distribution of either minimum relative bow displacement or relative bow velocity. For example, the top whiskers in groups 2 and 3 show little differences in Figure 14, indicating that group 2 bow entry events could be easily misclassified as group 3 or vice versa. This is an important consideration as minimum relative bow displacement is

often considered as the only parameter in the simulation of wet-deck slamming occurrences of WPCs in a seaway. Such an approach can be, to a certain degree, misleading in terms of the rate of slamming occurrences if only one reference section is used.

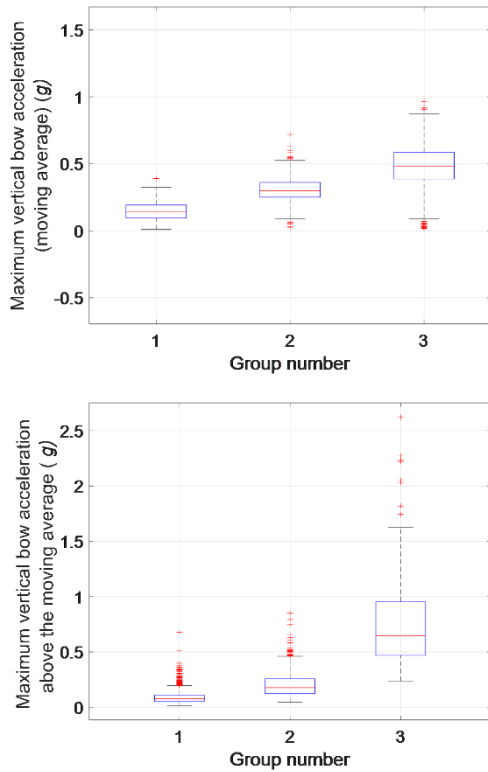


Figure 12: Box plot presentations of (top) maximum values of moving average of vertical bow acceleration during bow entry (*var1*) (bottom) maximum vertical bow acceleration above the moving mean (*var2*). Groups 1, 2 and 3 were determined by k-means ++ algorithm with input variables shown in Table 5.

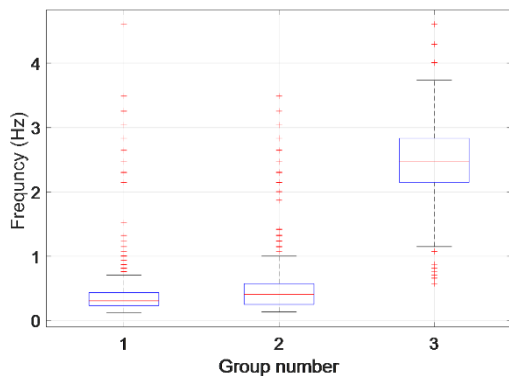


Fig13.a

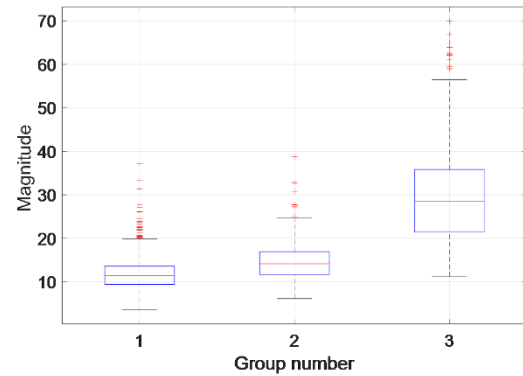


Fig13.b

Figure 13: Box plot presentations of (a) frequency with maximum magnitude in the wavelet transform during bow entry (*var3* in Table 5) and (b) wavelet transform maximum magnitude during bow entry (*var4* in Table 5), where raw data obtained from a strain gauge at Fr 61. Groups 1, 2 and 3 were determined by k-means ++ algorithm with input variables shown in Table 5.

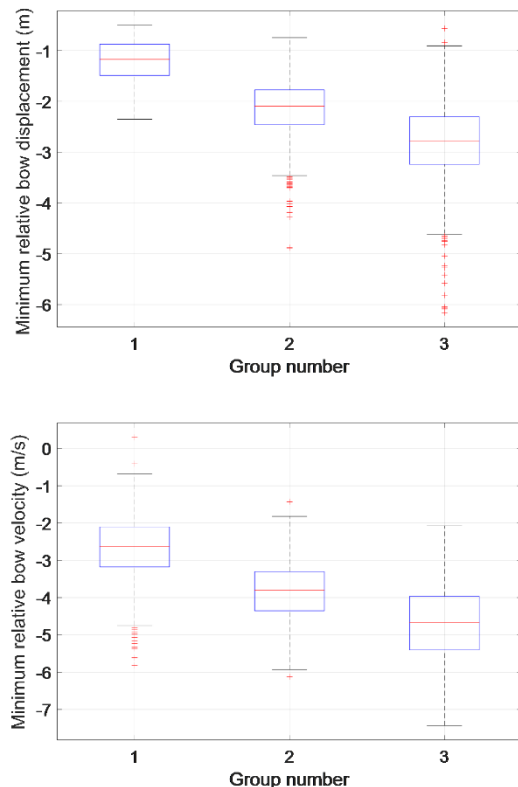


Figure 14: Box plot presentations of (top) minimum relative bow displacement (*var5* in Table 5) (bottom) minimum relative bow velocity (*var6* in Table 5). Groups 1, 2 and 3 were determined by k-means ++ algorithm with input variables shown in Table 5.

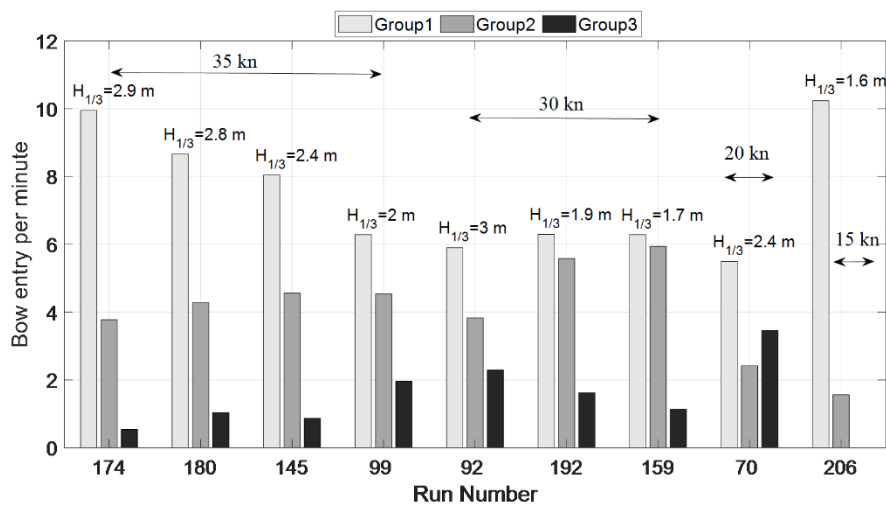


Figure 15 The rate of bow entry per minute for various groups for each individual run (refer to Table 4).

Figure 15 shows bow entry event rates for various runs at different speeds and significant wave heights. It can be seen that the bow entry event rates in group 2 can be several times higher than that in group 3. Interestingly, the results in Figure 15 show that in 30 and 20 knots the rates of group 3 bow entry events are higher than that in 35 knots, but such events are eliminated at a speed of 15 knots, highlighting the importance of effective speed reduction for decreasing the rate or minimising the likelihood of wet-deck slamming occurrences from operational perspective.

4.2 CLASSIFICATION OF BOW ENTRY EVENTS USING SUPERVISED LEARNING

Considering minimum relative bow displacement and velocity as a pair to classify bow entry events may lead to a better estimation of group 3 bow entry events in comparison to a single parameter criterion such as threshold relative vertical bow displacement. This is in fact a common approach for evaluating bottom slamming occurrences and the probability of such events in monohulls (Dessi and Ciappi, 2013). However, it should be noted that the conditions in which bottom entry events are classified for monohulls as either “slamming” or “no slamming” are usually defined by certain kinematics rules (Ochi and Motter, 1973) rather than by a data driven approach taken in the present work.

One approach for the classification of centre bow entry events could be to calculate distances from the centroid of each group shown in Figure 16 to determine the type of bow entry events. More broadly, supervised learning classification algorithms such as support vector machines (SVMs), naïve Bayes or decision trees can be applied. The full explanation of supervised learning

models and their applications for the classification of the bow entry events is beyond the scope of the present work but it is of interest to show how these models would generalise the bow entry classification problem by considering bow entry groups, shown in Figure 16, as training examples. An overview of possible outcomes from these models is presented in Figure 17. Table 6 shows the confusion matrix and the accuracy of these models with MATLAB’s default settings (version 2019a) for each algorithm.

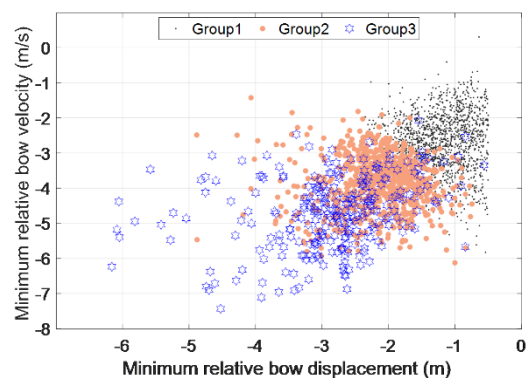
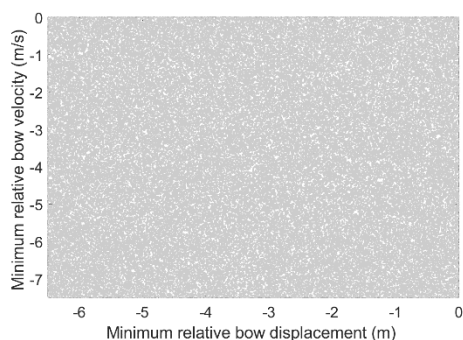


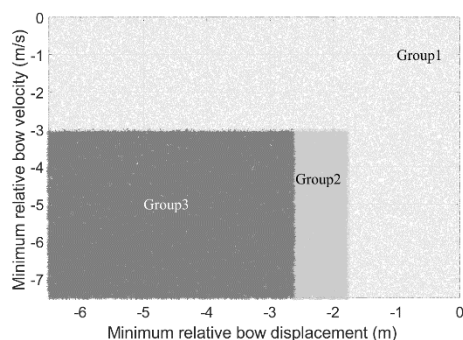
Figure 16 Minimum relative bow displacement versus minimum relative bow velocity during bow entry events in groups 1, 2 and 3.

Each algorithm resulted in a different pattern although the data used for training were identical. Figure 17(c) shows the result of a coarse decision tree which indicates a minimum relative displacement and velocity of about -2.6 m and -3 m/s for group 3 bow entry events, where the former value is comparable to the wet-deck clearance of Hull 061 in calm water and the latter is about 15% of a full speed of 38 knots. In contrast, at a relative displacement of -2.6 m, the two other models (i.e. linear

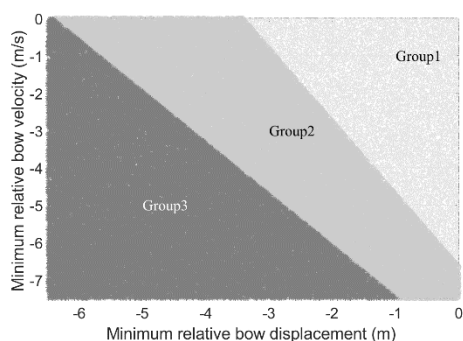
SVM and Gaussian naïve Bayes) shown in Figure 17 (a & b), suggest a relative bow velocity of - 5.3 m/s although these models describe the bow entry events quite differently in other regions.



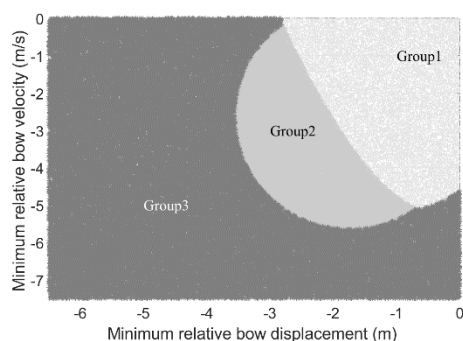
(a) Unclassified domain



(c) Classification based on a coarse decision tree



(b) Classification based on a linear support vector machine (SVM) model

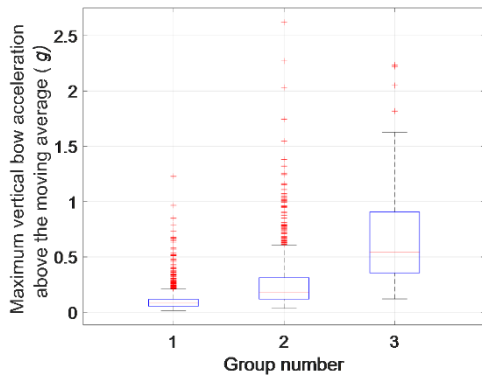


(d) Classification based on a Gaussian naïve Bayes model

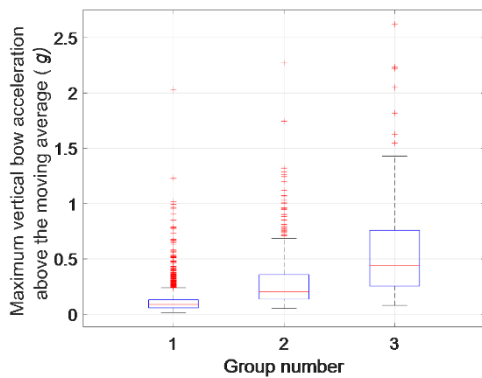
Figure 17 An overview of bow entry classification using three supervised learning models by incorporating data shown in Figure 16 as training examples.

Table 6 Confusion matrix and accuracy of trained models

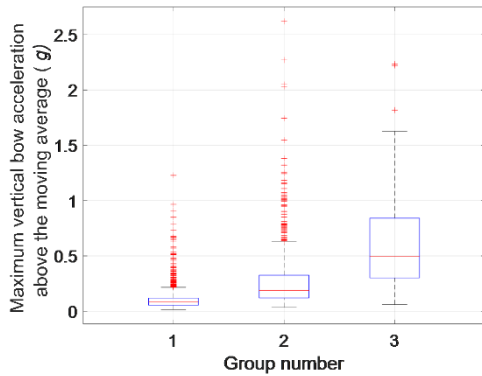
	Model 1	Model 2	Model 3																																																
Confusion matrix (observations)	<p>Model : Linear SVM</p> <table border="1"> <tr> <td>1</td> <td>1292</td> <td>80</td> <td></td> </tr> <tr> <td>2</td> <td>83</td> <td>615</td> <td>42</td> </tr> <tr> <td>3</td> <td>14</td> <td>139</td> <td>113</td> </tr> <tr> <td></td> <td>1</td> <td>2</td> <td>3</td> </tr> </table>	1	1292	80		2	83	615	42	3	14	139	113		1	2	3	<p>Model : Coarse Tree</p> <table border="1"> <tr> <td>1</td> <td>1327</td> <td>45</td> <td></td> </tr> <tr> <td>2</td> <td>250</td> <td>397</td> <td>93</td> </tr> <tr> <td>3</td> <td>29</td> <td>113</td> <td>124</td> </tr> <tr> <td></td> <td>1</td> <td>2</td> <td>3</td> </tr> </table>	1	1327	45		2	250	397	93	3	29	113	124		1	2	3	<p>Model : Gaussian Naive Bayes</p> <table border="1"> <tr> <td>1</td> <td>1307</td> <td>62</td> <td>3</td> </tr> <tr> <td>2</td> <td>113</td> <td>573</td> <td>54</td> </tr> <tr> <td>3</td> <td>16</td> <td>134</td> <td>116</td> </tr> <tr> <td></td> <td>1</td> <td>2</td> <td>3</td> </tr> </table>	1	1307	62	3	2	113	573	54	3	16	134	116		1	2	3
	1	1292	80																																																
	2	83	615	42																																															
	3	14	139	113																																															
	1	2	3																																																
1	1327	45																																																	
2	250	397	93																																																
3	29	113	124																																																
	1	2	3																																																
1	1307	62	3																																																
2	113	573	54																																																
3	16	134	116																																																
	1	2	3																																																
Accuracy	84.9 %	77.7%	83.9%																																																



(a) Model 1 groups: linear support vector machine (SVM)



(b) Model 2 groups: coarse decision tree



(c) Model3 groups: Gaussian Naive Bayes model

Figure 18 Box plot presentations of maximum vertical bow acceleration above the moving mean (*var2*) based on the outputs of three different classifiers trained by incorporating data shown in Figure 16 as training examples and general patterns described in Figure 17.

Moreover, the number of strong wet-deck slamming events in each group was found to be very different to that seen in the original groups used for training. This is shown in Figure 18 which shows the maximum bow vertical acceleration above the moving mean, or feature defined as *var2*, for each group for the three classifiers. As can be seen in Figure 18 (a-c), there are many outliers suggesting wet-deck slamming events in groups 1 and 2

as opposed to that seen in Figure 12 (b). Thus, it is difficult to judge whether wet-deck slamming events are best described by these classifiers without prior knowledge about the distribution of wet-deck slamming events in each group. Therefore, a probabilistic description of wet-deck slamming events is required.

4.3 PROBABILITY OF SLAMMING

The probability of wet-deck slamming $P(\text{slam})$ can be estimated as:

$$P(\text{slam}) = \frac{N_s}{N_{be}} = \frac{\sum_{i=1}^k N_{S,i}}{\sum_{i=1}^k N_{be,i}} \quad (1)$$

$$= \frac{\sum_{i=1}^k P_i \cdot N_{be,i}}{\sum_{i=1}^k N_{be,i}}$$

where, N_s is the total number of wet-deck slams, N_{be} is the total number of bow entry events, $N_{S,i}$ is the number of wet-deck slams in cluster i , $N_{be,i}$ is the number of bow entry events in cluster i , and P_i is wet-deck slamming probability of cluster i .

The number of bow entries for each cluster, $N_{be,i}$, in a seaway is a parameter that can be obtained through an ML model by considering a set of known features. What is difficult to estimate is the probability of wet-deck slamming for each cluster (P_i). The ideal situation is to find clusters in which P_i is the element of an ideal set, for example, clusters with $P_i \in \{1, 0\}$. This could be the case to a certain degree if the bow vertical acceleration and the wavelet features were used in an ML model such as the unsupervised model discussed in Section 4.1. As mentioned, such model is useful for automated data analyses for a monitoring system as described in Figure 7.

For simulation purposes, relative motions are considered as features to determine the rate of wet-deck slamming occurrences, in which P_i should be estimated for each cluster.

It is worth noting that, in the case of bottom slamming of monohulls, the assumption is that relative displacement and velocity are two features that describe “slamming” and “non-slamming” zones (Dessi, 2014, Dessi and Ciappi, 2013, Ochi and Motter, 1973), which means there exist two clusters with $P_1 \cong 1$ for slamming events and $P_2 \cong 0$ for non-slamming events. However, this was not the case in Figure 18 (a-c) and a broader approach should be developed.

One approach to estimate P_i for clusters could be based on empirical cumulative distribution probability of a third-party feature which can describe the severity of

slamming, such as maximum vertical bow acceleration during the bow entry or maximum vertical bow acceleration above the moving mean. Figure 19 shows cumulative probability plots of maximum vertical bow acceleration above the moving mean in three different groups obtained from the linear SVM classification model, which compares the cumulative probability at an arbitrary reference value of 0.5 g. The cumulative probability of bow entry with a figure above this can be calculated as an estimate for P_i for each cluster, which are approximately, 0.01, 0.13 and 0.53 for groups 1, 2 and 3 respectively. Table 7 shows the estimations of P_i for each cluster for the three models trained.

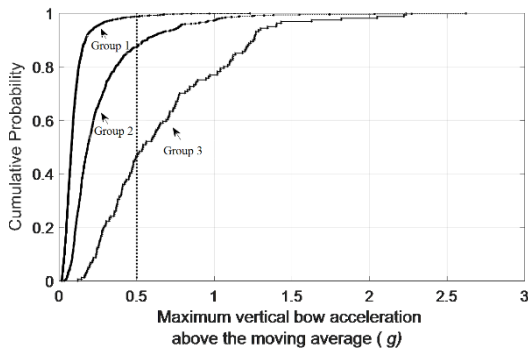


Figure 19 cumulative probability plots of max vertical bow acceleration above the moving mean in three different groups obtained from Model 1 classification algorithm (linear support vector machine (SVM)).

As can be seen in Table 7, wet-deck slamming events are less likely to occur in groups 1 and 2 compared to

Table 7 Empirical estimators of wet deck slamming probability (above given thresholds) in each group for different trained models with two thresholds of 0.5 g and 1 g for Hull 061 in head seas.

	Group 1	Group 2	Group 3	Group 1	Group 2	Group 3
threshold	0.5 g			1 g		
Model1	0.013	0.130	0.530	0.001	0.032	0.250
Model2	0.016	0.150	0.440	0.002	0.052	0.190
Model3	0.013	0.140	0.490	0.001	0.037	0.220

5. CONCLUSIONS

A remote hull monitoring system was developed for a 111 m catamaran with the objective of connectivity to a cloud-based platform in which machine learning/deep learning models could be deployed, enabling near real time analyses, classification and visualisation of data. The monitoring system is capable of measuring strain across multiple locations, bow and passenger deck accelerations, motions (i.e. heave, pitch and roll) and motions at the bow area relative to the water surface.

group 3 for each model. Although the choice of model does affect the probability of slamming for each group (i.e. P_i), the number of bow entries in each group (i.e. $N_{be,i}$) predicted by each model will change proportionally, and therefore $\sum_{i=1}^k P_i \cdot N_{be,i}$ is expected to be similar. Consequently, given a certain threshold (e.g. 0.5 g or 1 g) the choice of clustering should not significantly change the probability of slamming $P(\text{slam})$, which is equivalent to $\frac{\sum_{i=1}^k P_i \cdot N_{be,i}}{\sum_{i=1}^k N_{be,i}}$ as defined in Equation 1.

It is worth noting that the number and type of clusters can be important for optimal decision making, for instance to decide how often and to what degree the ship speed is required to be reduced in order to lower the probability of experiencing slamming events above a certain threshold in terms of slam-induced acceleration. However, recommending an optimal ship speed requires a much more complex matrix as other operational factors will come into effect.

The applicability of the presented method for monohull slamming has not been investigated and is thus a limitation of this work. Whether data driven methods for peak vertical acceleration distributions (Begovic *et al.*, 2016, Razola *et al.*, 2016, VanDerwerken and Judge, 2017) could be combined with appropriate ML models for improved slamming analyses is yet to be considered.

Using sea trials data available from a similar vessel (Hull 061) and with the consideration of both unsupervised and supervised learning algorithms, centre bow entry events were classified into different groups and the likelihood of wet-deck slamming in head seas was estimated in each group for slamming events above two slam-induced bow acceleration thresholds of 0.5 g and 1 g. By collecting a large amount of data of bow entry and wet-deck slamming events in various operational conditions, the models and estimates could be improved, and the probability of wet-deck slamming events in each cluster can be better evaluated. The ML approach

proposed in this paper can be used for clustering and grouping bow entry events. This also provides a basis for slamming probability analyses in each group/cluster for real-time operations. For instance, the effect of speed changes on relative motions and slamming probability in any sea state could be monitored and displayed, provided that the vessel is equipped with the appropriate sensors. Loads and motions information could be also used for future design analyses investigating the influence of wet-deck slamming.

More investigations are recommended to explore the application of learning models and recommendation systems for slamming, seakeeping, passenger comfort and the development of smart and connected hull monitoring systems such as on Incat Hull 093 and future WPC vessels to help with the improvement of high-speed vessels and the understanding of structural loads and sea keeping performance.

6. ACKNOWLEDGEMENTS

This work was undertaken in collaboration between the University of Tasmania, Revolution Design, Incat Tasmania, University of New South Wales Sydney, Italian National Research Council and University College London through the support of the Australian Research Council Linkage Grant number LP170100555. The work of Mr. Pete Woodward in the development of the hull monitoring system is also gratefully acknowledged.

7. REFERENCES

1 AGHABOZORGI, S., SHIRKHORSHIDI, A. S. & WAH, T. Y. 2015. *Time-series clustering—a decade review*. Information Systems, 53, 16-38.

2 ALAVIMEHR, J., LAVROFF, J., DAVIS, M. R., HOLLOWAY, D. S. & THOMAS, G. A. 2019. *An experimental investigation on slamming kinematics, impulse and energy transfer for high-speed catamarans equipped with ride control systems*. Ocean Engineering, 178, 410-422.

3 AMIN, W., DAVIS, M., THOMAS, G. & HOLLOWAY, D. 2013. *Analysis of wave slam induced hull vibrations using continuous wavelet transforms*. Ocean Engineering, 58, 154-166.

4 ARTHUR, D. & VASSILVITSKII, S. *K-means++: The advantages of careful seeding*. Proceedings of the eighteenth annual ACM-SIAM symposium on Discrete algorithms, 2007. Society for Industrial and Applied Mathematics, 1027-1035.

5 BEGOVIC, E., BERTORELLO, C., PENNINO, S., PISCOPO, V. & SCAMARDELLA, A. 2016. *Statistical*

analysis of planing hull motions and accelerations in irregular head sea. Ocean Engineering, 112, 253-264.

6 BEKKER, A. *Exploring the blue skies potential of digital twin technology for a polar supply and research vessel*. Proceedings of the 13th International Marine Design Conference Marine Design XIII (IMDC 2018), 2018. 135-146.

7 BERKHIN, P. 2006. *A survey of clustering data mining techniques. Grouping multidimensional data*. Springer, Berlin, Heidelberg.

8 BEZDEK, J. C. 1981. *Pattern recognition with fuzzy objective function algorithms*, New York, NY, US, Plenum Press.

9 DAVIS, M., FRENCH, B. & THOMAS, G. 2017. *Wave slam on wave piercing catamarans in random head seas*. Ocean Engineering, 135, 84-97.

10 DESSI, D. 2014. *Whipping-based criterion for the identification of slamming events*. International Journal of Naval Architecture and Ocean Engineering, 6, 1082-1095.

11 DESSI, D. & CIAPPI, E. 2013. *Slamming clustering on fast ships: From impact dynamics to global response analysis*. Ocean Engineering, 62, 110-122.

12 DUNN, J. C. 1973. *A fuzzy relative of the isodata process and its use in detecting compact well-separated clusters*. J. Cybernetics 3, 32– 57.

13 JACOBI, G., THOMAS, G., DAVIS, M., HOLLOWAY, D., DAVIDSON, G. & ROBERTS, T. 2012. *Full-scale motions of a large high-speed catamaran: The influence of wave environment, speed and ride control system*. International Journal of Maritime Engineering, 154, A143-A155.

14 JACOBI, G., THOMAS, G., DAVIS, M. R. & DAVIDSON, G. 2014. *An insight into the slamming behaviour of large high-speed catamarans through full-scale measurements*. Journal of Marine Science and Technology, 19, 15-32.

15 JAIN, A. K. 2010. *Data clustering: 50 years beyond k-means*. Pattern recognition letters, 31, 651-666.

16 JAIN, A. K. & DUBES, R. C. 1988. *Algorithms for clustering data*, Upper Saddle River, NJ, US, Prentice-Hall, Inc.

17 JAIN, A. K., MURTY, M. N. & FLYNN, P. J. 1999. *Data clustering: A review*. ACM computing surveys (CSUR), 31, 264-323.

18 KHAN, S. S. & AHMAD, A. 2004. *Cluster center initialization algorithm for k-means clustering*. Pattern recognition letters, 25, 1293-1302.

19 KUBAT, M. 2017. *An introduction to machine learning*, New York, NY, US, Springer-Verlag.

- 20 LAVROFF, J. & DAVIS, M. R. 2015. *Slamming kinematics, impulse and energy transfer for wave-piercing catamarans*. Journal of Ship Research, 59, 145-161.
- 21 LAVROFF, J., DAVIS, M. R., HOLLOWAY, D. S. & THOMAS, G. 2013. *Wave slamming loads on wave-piercer catamarans operating at high-speed determined by hydro-elastic segmented model experiments*. Marine structures, 33, 120-142.
- 22 LAVROFF, J., DAVIS, M. R., HOLLOWAY, D. S., THOMAS, G. A. & MCVICAR, J. J. 2017. *Wave impact loads on wave-piercing catamarans*. Ocean Engineering, 131, 263-271.
- 23 LIKAS, A., VLASSIS, N. & VERBEEK, J. J. 2003. *The global k-means clustering algorithm*. Pattern recognition, 36, 451-461.
- 24 LLOYD, S. 1982. *Least squares quantization in pcm*. IEEE transactions on information theory, 28, 129-137.
- 25 MAGOGA, T., AKSUS, S., CANNON, S., OJEDA, R. & THOMAS, G. 2017. *Identification of slam events experienced by a high-speed craft*. Ocean Engineering, 140, 309-321.
- 26 MAHDAVINEJAD, M. S., REZVAN, M., BAREKATAIN, M., ADIBI, P., BARNAGHI, P. & SHETH, A. P. 2018. *Machine learning for internet of things data analysis: A survey*. Digital Communications and Networks, 4, 161-175.
- 27 MCVICAR, J., LAVROFF, J., DAVIS, M. R. & THOMAS, G. 2018. *Fluid-structure interaction simulation of slam-induced bending in large high-speed wave-piercing catamarans*. Journal of Fluids and Structures, 82, 35-58.
- 28 MITRA, M. & GOPALAKRISHNAN, S. 2016. *Guided wave based structural health monitoring: A review*. Smart Materials and Structures, 25, 053001.
- 29 OCHI, M. K. & MOTTER, L. E. 1973. *Prediction of slamming characteristics and hull responses for ship design*. Trans. SNAME, 81, 144-176.
- 30 RAZOLA, M., OLAUSSON, K., GARME, K. & ROSÉN, A. 2016. *On high-speed craft acceleration statistics*. Ocean Engineering, 114, 115-133.
- 31 SHABANI, B., HOLLOWAY, D., LAVROFF, J., DAVIS, M. & THOMAS, G. *Systematic model tests on centre bow design for motion and slamming load alleviation in high speed catamarans*. 14th international conference on fast sea transportation, 2017 Nantes, France. 136-143.
- 32 SHABANI, B., LAVROFF, J., DAVIS, M. R., HOLLOWAY, D. S. & THOMAS, G. A. 2018a. *Slam loads and kinematics of wave-piercing catamarans during bow entry events in head seas*. Journal of Ship Research, 62, 134-155.
- 33 SHABANI, B., LAVROFF, J., DAVIS, M. R., HOLLOWAY, D. S. & THOMAS, G. A. 2019a. *Slam loads and pressures acting on high-speed wave-piercing catamarans in regular waves*. Marine Structures, 66, 136-153.
- 34 SHABANI, B., LAVROFF, J., HOLLOWAY, D. S., DAVIS, M. R. & THOMAS, G. A. 2018b. *The effect of centre bow and wet-deck geometry on wet-deck slamming loads and vertical bending moments of wave-piercing catamarans*. Ocean Engineering, 169, 401-417.
- 35 SHABANI, B., LAVROFF, J., HOLLOWAY, D. S., DAVIS, M. R. & THOMAS, G. A. 2019b. *Centre bow and wet-deck design for motion and load reductions in wave piercing catamarans at medium speed*. Ships and Offshore Structures, 1-17.
- 36 SHABANI, B., LAVROFF, J., HOLLOWAY, D. S., DAVIS, M. R. & THOMAS, G. A. 2019c. *The influence of the centre bow and wet-deck geometry on motions of wave-piercing catamarans*. Proceedings of the Institution of Mechanical Engineers, Part M: Journal of Engineering for the Maritime Environment, 233, 474-487.
- 37 SHABANI, B., LAVROFF, J., HOLLOWAY, D. S., DAVIS, M. R. & THOMAS, G. A. 2019d. *Wet-deck slamming loads and pressures acting on wave piercing catamarans*. International Shipbuilding Progress, 66, 201-231.
- 38 SINGH, A., YADAV, A. & RANA, A. 2013. *K-means with three different distance metrics*. International Journal of Computer Applications, 67.
- 39 THOMAS, G., WINKLER, S., DAVIS, M., HOLLOWAY, D., MATSUBARA, S., LAVROFF, J. & FRENCH, B. 2011. *Slam events of high-speed catamarans in irregular waves*. Journal of Marine Science and Technology, 16, 8-21.
- 40 VANDERWERKEN, D. & JUDGE, C. 2017. *Statistical analysis of vertical accelerations of planing craft: Common pitfalls and how to avoid them*. Ocean Engineering, 139, 265-274.
- 41 WITTEN, I. H., FRANK, E., HALL, M. A. & PAL, C. J. 2016. *Data mining: Practical machine learning tools and techniques*, Cambridge, MA, US, Morgan Kaufmann.